Experimental Study of PCB Vibration Induced by MLCC Assembly Orientation and Process Variations

Yifan Ding¹, Ming-Feng Xue², Jianmin Zhang³, Xin Hua⁴, Benjamin Leung⁵, Eric A. MacIntosh⁶, Chulsoon Hwang⁷

EMC Laboratory, Missouri University of Science and Technology, Rolla, MO-65401, USA

dingyif@mst.edu¹, hwangc@mst.edu⁷

Google Inc., USA

mingfengx@google.com², jianmin@google.com³, xihua@google.com⁴, benleung@google.com⁵, ericmac@google.com⁶

Abstract— The piezoelectric effect will cause the multilayer ceramic capacitor (MLCC) to deform in several directions. When it is soldered to the printed circuit board (PCB) and powered on, these deformations will exert a certain force on the PCB, causing the PCB to vibrate and emit acoustic noise at a certain frequency. Determining the dominant deformation direction that MLCC can affect the PCB is relevant and important for efficiently extracting the equivalent source of noise. This paper provides a method to determine the dominant deformation direction produced by MLCC, explores it through experimental measurement results, and finally provides a conclusion to the investigation.

Keywords—Multilayer ceramic capacitor (MLCC), power noise, piezoelectric characteristic, deformation, equivalent source, vibration velocity

I. INTRODUCTION

Multilayer ceramic capacitors (MLCCs) are widely used due to its compact size, high capacitance density, and small equivalent series inductance. When subjected to an alternating electric field, an MLCC undergoes elastic deformation due to the piezoelectric effect, as depicted in Fig. 1. The expansion and contraction of the MLCC occur parallel and perpendicular to the electrode sheet plane in response to changes in the electric field. As the MLCC is soldered onto the printed circuit board (PCB), its deformation acts as an equivalent source of excitation, inducing vibrations in the PCB [1] - [2]. In cases where the noise frequency falls within the audible range, the resultant PCB vibration is prone to generating audible noise. Specifically, if the noise frequency aligns with the self-resonant frequency of the PCB and the MLCC is situated in an area with pronounced selfresonance deformations, the PCB's vibration velocity experiences a significant increase. This heightened vibration results in discernible acoustic noise at that particular frequency.

Previous studies have focused on characterizing the noise issues caused by MLCC. Simulation and measurement methods for identifying PCB vibration and "singing" problems were proposed in [3] and [4]. In [5], a study introduced an automated process for noise simulation. In the investigation of the MLCC excitation mechanism [6], the electromechanical material properties of the MLCC were determined to reveal the fundamental causes of MLCC deformation. The research in [7] modeled MLCC excitation as a force perpendicular to the PCB over the entire encapsulation area where the MLCC is located. To dive deeper into the details, in [1], modal analysis was conducted for surface deformation measurements of MLCC. However, due to the small size of the MLCC, the natural

This work was supported in part by the National Science Foundation (NSF) under Grant IIP-1916535.

frequency of the MLCC is much beyond the human audible frequency (20 Hz to 20 kHz). The analysis also indicates that the source can be represented by a force perpendicular to the mounting surface, a pair of forces parallel to the mounting surface, and a pair of moments.

However, assumptions about MLCC forces are based on a specific placement orientation, specifically, the orientation of the electrode plates inside the MLCC being parallel to the PCB's plane. Nevertheless, during actual soldering operations, the internal structure of MLCC is not easily observable. Additionally, in scenarios involving a large number of MLCCs that need to be soldered, individually inspecting the orientation of each MLCC is practically unfeasible. Therefore, in practical situations, there may be two different orientations of MLCC on the PCB, as shown in Fig. 2.

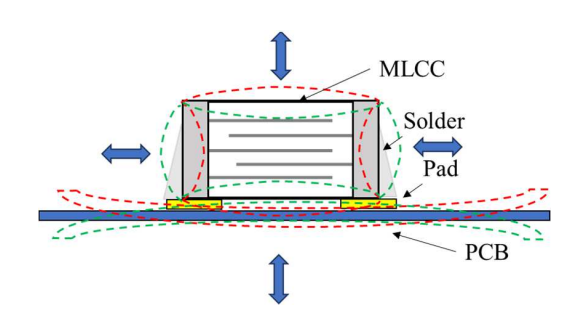


Fig. 1. MLCC deformation and its induced PCB vibration.

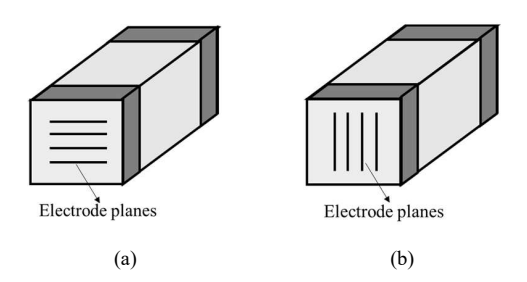


Fig. 2. Two possible orientations for MLCC placed on PCB. (a) Inner electrode planes parallel to the PCB surface. (b) Inner electrode planes perpendicular to the PCB surface.

In recent research [2], researchers proposed an equivalent force extraction method to quantify forces induced by electronic components, aiding in predicting the impact of MLCC on the system. This method can be extended to other forms of forces, laying the foundation for constructing a library of equivalent sources for MLCC-induced PCB vibrations. Given the present research emphasis, it is both captivating and imperative to determine whether the impact of MLCC on PCB vibrations is consistent under two placement scenarios, i.e., finding the dominant deformation direction of MLCC affecting PCB. Utilizing simulations to assess the influence of various MLCC assembly orientations on induced PCB vibrations is a valuable approach. The MLCC deformation pattern and its induced PCB vibration pattern can be simulated according to [1] and [2]. However, it presents challenges, such as the need to acquire accurate information on the size and material properties of the MLCC, which is often not readily available. Additionally, simulating these intricate structures is a time-intensive process. To address these challenges, an experimental-based method is proposed in this paper. This approach not only considers the influencing factors of MLCC orientation but also accounts for errors introduced during the soldering process—an integral step in the production and manufacturing process.

In this paper, a method is proposed to explore the dominant deformation direction of MLCC affecting PCB by measuring the MLCC-induced PCB vibration under different soldering orientations, and based on this method, conclusions were drawn by comparing the vibration amplitude under different conditions. The methods explored are presented in Section II, the measurement setup, results, and analysis in Section III, and the conclusions in Section IV.

II. DOMINANT DEFORMATION DIRECTION OF MLCC

To discern whether the force exerted by the MLCC on the PCB predominantly arises from the capacitor's deformation parallel or perpendicular to the PCB direction, the capacitor can be soldered onto the PCB pad in two distinct orientations. In one scenario, the electrode plate inside the capacitor was assumed to align parallel to the PCB plane, as displayed in Fig. 2 (a). In the other scenario, the electrode plate inside the capacitor was assumed perpendicular to the PCB plane, as illustrated in Fig. 2 (b).

In the case of Fig. 2(a), the schematic diagram of the deformation of the MLCC induced by powering is shown in Figure 3(a)-(b). The diagram represents a front view, revealing the solder pads on the PCB (highlighted in the yellow area), the internally interleaved electrode plates of the MLCC, and the deformations of the MLCC. In Fig. 3 (a), the MLCC extends vertically to the PCB and electrode plate direction while contracting in the direction perpendicular to the two terminals of the MLCC (red dashed line). In Fig. 3 (b), the MLCC contracts vertically to the PCB and electrode plate direction while extending in the direction perpendicular to the two terminals of the MLCC (green dashed line). Deformations in both directions exert a certain force on the PCB. Similarly, in the case of Fig. 2(b), the schematic diagram of the MLCC deformation is shown in Fig. 3(c)-(d). The diagram represents a top view, illustrating the solder pads on the PCB (highlighted in the yellow area), the internally interleaved electrode plates of the MLCC, and the deformations of the MLCC. In Fig. 3(c), the MLCC extends parallel to the PCB and vertically to the electrode plate direction while contracting in the direction perpendicular to the two terminals of the MLCC (red dashed line). In Fig. 3(d), the MLCC contracts parallel to the PCB and vertically to the

electrode plate direction while extending in the direction perpendicular to the two terminals of the MLCC (green dashed line).

If the vibration amplitudes of the PCB resulting from the MLCC are relatively similar under both soldering orientations, it implies that the force influencing the PCB primarily originates from the capacitor's deformation perpendicular to the two terminals of the MLCC. Conversely, disparate amplitudes suggest that the MLCC's impact on the PCB primarily stems from the capacitor's deformation perpendicular to the MLCC electrode plates.

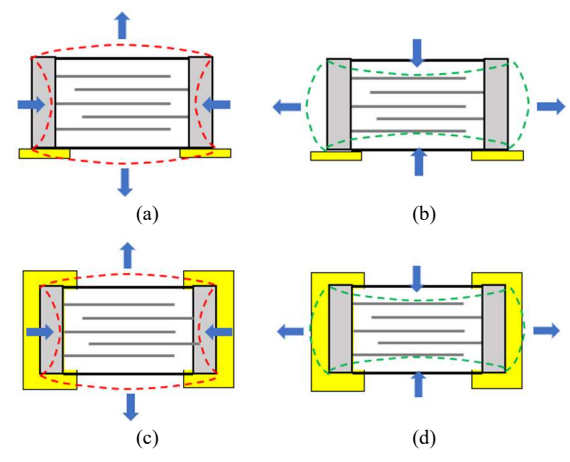


Fig. 3. MLCC deformation direction for two soldering orientations. Solder pads are highlighted in the yellow area. (a) the MLCC extends vertically to the PCB and electrode plate direction while contracting in the direction perpendicular to the two terminals of the MLCC (red dashed line). (b) the MLCC contracts vertically to the PCB and electrode plate direction while extending in the direction perpendicular to the two terminals of the MLCC (green dashed line) (c) the MLCC extends parallel to the PCB and vertically to the electrode plate direction while contracting in the direction perpendicular to the two terminals of the MLCC (red dashed line). (d) the MLCC contracts parallel to the PCB and vertically to the electrode plate direction while extending in the direction perpendicular to the two terminals of the MLCC (green dashed line)

III. EXPERIMENTAL INVESTIGATION

The direct expression of the force exerted by the MLCC on the PCB can be observed through the vibrations induced in the PCB under certain power supply conditions. Following the assessment method outlined in Section II, this section employs a measurement approach to investigate the primary deformation direction of the MLCC causing the vibration in the PCB.

A. Measurement Setup

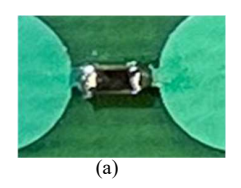
The PCB vibration measurement setup for the investigation utilizing a laser Doppler vibrometer (LDV) system was detailed in [2]. A two-layer PCB featuring a symmetric layout is employed as illustrated in Fig. 4, which has a lightweight design and is easily susceptible to small excitations. To secure the PCB, screws were applied to fix its four corners onto a heavy platform. One soldering location was positioned at the center of the top layer surface for a capacitor in 0603 package size. The soldering pads have dimensions of 0.88 mm \times 0.65 mm, with a center-to-center distance of 1.45 mm. Soldered onto these pads was an 0603 capacitor with a capacitance of 22 μF .

The power rail voltage maintained a 1 V DC offset, coupled with a sinusoidal ripple exhibiting a 1 V AC amplitude, spanning the frequency range of 200 Hz to 3000 Hz. The alternating power input induced deformation in the MLCC owing to the piezoelectric effect. This deformation served as the excitation source for PCB vibration, aligning with the frequency of the supply voltage. The velocity of PCB vibration is gauged from an observation point denoted by a red dot in Fig. 4.



Fig. 4. Test vehicle PCB for vibration measurement. The red dot represents the location for observing the PCB vibration velocity.

The method to determine in which direction the deformation of the MLCC is the main cause of PCB vibration has been provided in Section II. However, the orientation of the internal electrode plates of the MLCC is unknown during the actual soldering process. To address this ambiguity, one side of the MLCC was marked black. Consequently, these two soldering methods can be visualized in Fig. 5 (a) and (b) during the measurement process. Recognizing potential errors introduced by factors like capacitor position and solder height during repeated soldering, four sets of tests were conducted to characterize the measured run-to-run variation. In the first round of measurement, the black side of the MLCC faced towards the top. In the second round of measurement, the MLCC was turned by 90 degrees, and the black side was faced towards the front. In the third round, the MLCC was turned back by 90 degrees and the black side was towards the top again, as in the first round. Finally, in the fourth round, the MLCC's orientation was the same as the second round.



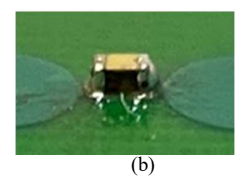


Fig. 5. Two orientations for MLCC soldering. (a) Black side facing the top side. Applied in round 1 and round 3. (b) Black side facing the front side. Applied in round 2 and round 4.

B. MLCC-Induced PCB Vibration Comparison

The PCB vibration velocities measured at the observation point during the four rounds within the specified frequency range are depicted in Fig. 6. An area of particular concern arises due to notably elevated vibration velocities at specific frequencies. This is a significant concern, as higher vibration velocities carry an increased likelihood of contributing to pronounced acoustic noise issues. The frequencies exhibiting

these elevated velocities are denoted as modes 1 through 5 in Fig. 6. A comprehensive understanding of the definition of "mode" in the context of PCB vibration, along with the corresponding vibration velocity amplitudes at each mode, is available in [2]. It is crucial to clarify that the numbers marked in Fig. 6 do not correspond to real mode numbers but rather signify several modes that have been the focal point of this investigation. Table I provides a detailed overview of the vibration speeds associated with these highlighted modes.

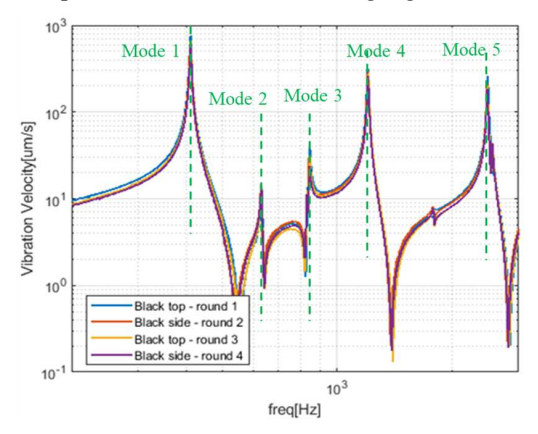


Fig. 6. PCB vibration velocities observed in the four rounds.

TABLE I. PCB VIBRATION VELOCITY (UM/S) AT THE OBSERVATION POINT AT THE FOCUSED MODES FOR THE FOUR ROUNDS

	Mode 1	Mode 2	Mode 3	Mode 4	Mode 5
Round 1	754.19	11.545	38.19	313.40	259.96
Round 2	647.62	13.951	30.622	286.17	211.03
Round 3	664.64	13.322	30.757	273.96	199.63
Round 4	607.65	14.539	23.656	258.88	184.61

TABLE II. PCB VIBRATION VELOCITY DIFFERENCE BETWEEN DIFFERENT ROUNDS AT THE FOCUSED MODES

Difference between	Mode 1	Mode 2	Mode 3	Mode 4	Mode 5
Round 1 2	14.13%	-20.84%	19.81%	8.68%	18.82%
Round 2 3	-2.62%	4.50%	-0.44%	4.26%	5.40%
Round 3 4	8.57%	-9.13%	23.08%	5.50%	7.52%
Round 1 3	11.87%	-15.39%	19.46%	12.58%	23.20%
Round 2 4	6.17%	-4.21%	22.74%	9.53%	12.51%

The data presented in Fig. 6 reveals a consistent trend in the PCB vibration speed measured at the observation point across the four measurement rounds across the entire frequency range of interest. This consistency is further emphasized in Table I, where the vibration amplitude at the mode with a relatively high amplitude exhibits a similar pattern. At the same mode, the vibration speeds measured in the four rounds are remarkably

close. This point is further underscored by the comparative analysis in Table II. Table II delineates the differences in PCB vibration velocity between different measurement rounds, particularly at the identified focused modes. In the first three rows, the comparison details the variance in vibration velocity at the same mode in consecutive test rounds. This disparity indicates the force change resulting from alterations in the direction of the capacitor plate following a reorientation of MLCC placement, alongside uncontrollable run-to-run variations stemming from the re-soldering process. The last two lines specifically highlight the difference in vibration speed of the capacitor before and after re-soldering when the electrode planes of the MLCC maintain the same orientation. This difference solely encapsulates variations introduced by the soldering process.

Examining the data in Table II reveals that, for the same MLCC orientation, the alteration in the vibration velocity induced by re-soldering the capacitor within the frequency range of interest remains within a 25% range. This observed change is deemed reasonable, as it encompasses various factors, including the displacement of the capacitor before and after the two soldering instances, as well as the variations in solder quantity leading to differences in the height and tilt angle of the capacitor relative to the PCB during the soldering process. As highlighted earlier, variations are inherent in the soldering process. Examining the differences between consecutive measurement rounds, the shifts in PCB vibration resulting from two distinct orientations of the MLCCs also fall within a 25% margin. When altering the orientation of the capacitor, changes in vibration speeds across different modes are as expected. Beyond the inherent errors in soldering and measurement processes, this variation encompasses shifts in force on the PCB stemming from the diverse directions of the electrode plates. However, the capacitor electrode plate direction change does not introduce additional differences. Thus, it can be concluded that this factor is not the primary cause of significant changes in the vibration amplitude. It can be further inferred that following capacitor welding to the pad, distinct orientations of the electrode plates engender diverse forces on the PCB. Yet, this disparity in forces

does not lead to substantial alterations in the vibration amplitude of the PCB.

IV. CONCLUSION

This paper provided a method to determine the dominant deformation direction produced by MLCC. The method was based on comparing the PCB vibration caused by the MLCC under two different soldering orientations. It was explored through PCB vibration measurement results under four rounds of tests. The experimental results show that the changing of MLCC assembly orientation and the soldering process leads to the PCB vibration varies within 25%, which is reasonably stable considering the measurement uncertainties. Conclusion of this study suggests that MLCC orientation does not affect much, so less attention is required in soldering process regarding the orientation.

REFERENCES

- BH. Ko, SG. Jeong, YG. Ahn, KS. Park, NC. Park, and YP. Park, Analysis of the correlation between acoustic noise and vibration generated by a multi-layer ceramic capacitor. *Microsyst Technol* 20, 1671–1677 (2014).
- [2] Y. Ding et al., Equivalent Force Extraction Methodology for Electrical Component Induced PCB Vibration, in *IEEE Trans. Electromagn. Compat.*, vol. 66, no. 1, pp. 270-280, Feb. 2024.
- [3] Y. Sun, S. Wu, J. Zhang, C. Hwang, and Z. Yang, Measurement Methodologies for Acoustic Noise Induced by Multilayer Ceramic Capacitors of Power Distribution Network in Mobile Systems, in *IEEE Trans. Electromagn. Compat.*, vol. 62, no. 4, pp. 1515-1523, Aug. 2020.
- [4] Y. Sun, S. Wu, J. Zhang, C. Hwang, and Z. Yang, Simulation Methodologies for Acoustic Noise Induced by Multilayer Ceramic Capacitors of Power Distribution Network in Mobile Systems, in *IEEE Trans. Electromagn. Compat.*, vol. 63, no. 2, pp. 589-597, April 2021.
- [5] X. Yan et al., A Methodology for Predicting Acoustic Noise From Singing Capacitors in Mobile Devices, in *IEEE Trans. Electromagn. Compat.*, vol. 65, no. 4, pp. 1266-1270, Aug. 2023.
- [6] B. H. Ko, S. Jeong, D. Kim, N. C. Park, and Y. P Park, Identification of the electromechanical material properties of a multilayer ceramic capacitor. *Int. J. Appl. Ceram* 14, no. 3 (2017): 424-432.
- [7] Y. Ding et al., Extraction for Multilayer Ceramic Capacitor Vibration Induced Force, 2023 IEEE Symposium on Electromagnetic Compatibility & Signal/Power Integrity (EMC+SIPI), Grand Rapids, MI, USA, 2023, pp. 115-119.